Mechanism of Intermembrane Phosphatidylcholine Transfer: Effects of pH and Membrane Configuration†

Eungyeong Yang and Wray H. Huestis*

Department of Chemistry, Stanford University, Stanford, California 94305

Received May 20, 1993; Revised Manuscript Received August 13, 1993•

ABSTRACT: The mechanism of phospholipid transfer between membranes has been studied as a function of the configuration and concentration of donor and recipient membranes. The study was motivated by the observation that dimyristoylphosphatidylcholine transfers from sonicated vesicles to erythrocytes at a 4-fold faster rate at pH 5.5 than at pH 7.4. It is unexpected that the solubility of phosphatidylcholine should be affected by pH changes in this range; indeed, the more hydrophilic homolog dilauroylphosphatidylcholine transfers at closely similar rates at pH 5.5 and 7.4. The behavior of the more hydrophobic lipid is not consistent with transfer solely as a monomer passing through the aqueous phase. The effects of membrane proximity on phospholipid transfer were examined in dilution experiments employing intact erythrocytes, resealed ghosts, erythrocyte membrane buds, and sonicated vesicles as both donor and recipient membranes. For both hydrophobic and less hydrophobic lipids, the kinetics of intermembrane transfer were affected significantly by dilution at constant donor:recipient ratios. The results were fit to a kinetic model containing contributions from both through-solution monomer transfer and transient collisional transfer. The model predicts that the mechanism of intermembrane transfer varies with experimental conditions such as membrane concentration, donor and acceptor membrane area, and surface curvature. Through-solution monomer transfer predominates for less hydrophobic lipids at all values of pH and membrane concentration, and for more hydrophobic lipids at very high membrane dilutions. Transient collisional transfer contributes significantly to the rate for relatively hydrophobic lipids in concentrated donor–acceptor systems, an effect that is particularly evident at pH values below 6. The size and surface configuration of donor and recipient membranes also alter the relative contributions of through-solution and collisional transfer.

The spontaneous intermembrane transfer of lipid molecules has been demonstrated in a variety of systems [for a recent review, see Brown (1992)]. Two principal mechanisms have been proposed for this ubiquitous phenomenon: through-solution monomer transfer and transfer during transient collisions. The majority of studies prior to 1988 had indicated that lipid molecules transfer as monomers through the aqueous phase (Papahadjopoulos et al., 1976; Martin & McDonald, 1976; Duckwitz-Peterlein et al., 1977; Roseman & Thompson, 1980; Nichols & Pagano, 1981, 1982; Mclean & Phillips, 1981, 1984a,b; DeCuyper et al., 1983, 1985; Arvinte & Hildenbrand, 1984). Only recently, some evidence supporting an additional concentration-dependent process has come from studies in phosphatidylcholine vesicles (Jones & Thompson, 1989) and mixed phosphatidylcholine–taurocholate micelles (Nichols, 1988). The former finding was attributed to an enhancement of the first-order process, presumably resulting from attractive interactions between transiently apposed bilayers and some fraction of the potentially desorbing lipid molecules (Jones & Thompson, 1990; Wimley & Thompson, 1991). In the latter case, the micellar collisional process presumably occurred via a fused complex, reducing the activation entropy (Fullington et al., 1990).

A previous study of phospholipid transfer from sonicated phospholipid vesicles to human erythrocytes (Ferrell et al., 1985b) showed that the rate of lipid transfer decreased exponentially with increasing acyl chain length. This acyl chain dependence likely reflects the energetics of monomer transfer through the aqueous phase. However, inconsistencies between the monomer transfer model and the observed kinetics were found for lipids that transfer slowly. According to the monomer transfer model, double-reciprocal plots (1/initial rate vs 1/[cell lipid] for various vesicle concentrations) should yield parallel lines, but the observed slopes of these lines varied systematically. This finding suggested two possible modifications of the monomer transfer model: caged monomer transfer between membranes, or an additional reaction pathway for lipid monomers. Both modified models predict nonparallel slopes in the double-reciprocal plots, but there was no basis for discriminating between them. Steck et al. (1988) also have proposed a mechanism similar to the caged monomer transfer model, in which the formation of an activated cholesterol molecule is required prior to a productive donor–acceptor collision.

The work described in this paper addresses the detailed mechanism of intermembrane phospholipid transfer between erythrocytes and vesicles. Since the kinetic criteria for monomer transfer are not satisfied for all circumstances [as discussed in Ferrell et al. (1985b)], we design experiments to characterize the monomer transfer model further. From the data gained here, we develop a new kinetic model which consists of two parts: monomer transfer and a transient collision term. This combined model rationalizes the kinetic observations for hydrophobic phosphatidylcholine transfer at pH 7.4, and provides insight into the effects of pH on this process.

MATERIALS AND METHODS

Materials. Dilauroylphosphatidylcholine (DLPC),[1] dimyristoyl-PC (DMPC), dioleoyl-PC (DOPC), dipalmitoyl-PC (DPPC), lysopalmitoyl-PC (lyso-PPC), dipalmitoylphosphatidylglycerol (DPPG), Pronase E (protease type XXV from *Streptomyces griseus*), neuraminidase (from *Clostridium*

† This work was supported by NIH Grant HL 23787.
* To whom correspondence should be addressed.
• Abstract published in *Advance ACS Abstracts,* October 15, 1993.

0006-2960/93/0432-12218$04.00/0

perfringens, type X), and bovine serum albumin (BSA) were purchased from Sigma Chemical Co. (St. Louis, MO); 1-palmitoyl-2-[9-(4,4-dimethyl-*N*-oxyoxazolidin-2-yl)stearoyl]-PC (spin PC) was from Avanti Polar Lipids, Inc. (Birmingham, AL); 4,4′-diisothiocyano-2,2′-stilbenedisulfonic acid (DIDS) was from Pierce Chemical Co. (Rockford, IL); [^{14}C]DPPC and [^{14}C]DMPC were from Amersham Corp. (Arlington Heights, IL). [^{14}C]DLPC was synthesized from dilauroylphosphatidylethanolamine (Sigma) and methyl iodide (Aldrich) plus [^{14}C]methyl iodide (Amersham Corp.) as described (Stockton et al., 1974; Ferrell et al., 1985a). All phospholipids were >98% pure by thin-layer chromatographic analysis. All other chemicals were of reagent grade.

Cells. Blood was obtained by venipuncture from healthy adult volunteers and collected in citrate anticoagulant. Erythrocytes were isolated from plasma and other cells by centrifugation for 5 min at 1800*g*, and washed 3–4 times with 4–10 volumes of 150 mM NaCl and twice with 4–10 volumes of NaCl/P_i (138 mM NaCl, 5 mM KCl, 1.4 mM NaH_2PO_4, 6.1 mM Na_2HPO_4, 1 mM $MgSO_4$, and 5 mM glucose, pH 7.4). Cells not used immediately were suspended in NaCl/P_i, stored at 4 °C, and used within 12 h of collection.

Alteration of Cell pH. Buffers with different pHs were prepared with MES or HEPES and various concentrations of NaCl and sucrose, designed to preserve normal cell volume (M. Gedde, personal communication). Cells were washed in buffer (pH 5.5 buffer, 155 mM NaCl/40 mM MES; pH 5.9 buffer, 140 mM NaCl/60 mM MES; pH 7.4 buffer, NaCl/P_i; pH 8.17 buffer, 64 mM NaCl/50 mM HEPES/62 mM sucrose) at 10% HCT 3 times with an incubation at room temperature for 5 min each. Cells were then used immediately.

Preparation of Vesicles. Lyso-PC micelles and small unilamellar PC vesicles were prepared by suspending lipid in buffer and sonicating the suspension in a bath sonicator to clarity. Thin-layer chromatographic analysis revealed no detectable (>0.1%) hydrolysis or oxidation products in vesicle samples. In some experiments, a ^{14}C-labeled analog of the appropriate lipid was incorporated by cosonication (typically 0.1–0.12 μCi/mL total vesicle lipid). Vesicles containing encapsulated Mn^{2+} were prepared as follows: using a probe sonicator (Heat Systems, Inc., Farmingdale, NY; Model XL2010), the DMPC suspension (100 mM) was sonicated first in the presence of 500 mM Mg^{2+} until almost transparent, in order to saturate nonspecific cation binding sites. Mn^{2+} was added to yield a concentration of 1 M, and the suspension was resonicated to clarity. A trace amount of [^{14}C]DPPC (0.01 μCi/mM total lipid) was included in the sonication medium as a vesicle marker. Sonicated vesicles were centrifuged at 30000*g* for 10 min to remove probe titanium particles. Excluded ions were then removed by three batch treatments with 0.6 volume of Chelex 100 resin (ion-exchange resin, Bio-Rad), followed by passage through a PD-10 column (Sephadex G-25M, Pharmacia) preequilibrated with pH 5.5 buffer. The final lipid concentration was determined by liquid scintillation counting, and the final concentration of Mn^{2+} encapsulated was calculated from the enclosed volume for sonicated vesicles [4.3% for 100 mM sonicated unilamellar DMPC vesicles 25 nm in diameter (Huang, 1969)] and the lipid recovery.

Preparation of Resealed Ghosts. Packed cells were lysed in 14 mM HEPES/2 mM $MgSO_4$, pH 7.4 (lysing buffer), at 4 °C. The membranes were pelleted by centrifugation at 12000*g* for 20 min, 4 °C, followed by additional washes in the lysing buffer until supernatants were free of detectable hemoglobin. Ghosts were resealed by adding 8 volumes of the lysing buffer containing 2 mM Mg-ATP, followed by 1 volume of 10× salt (1.38 M KCl, 100 mM NaCl, 20 mM $MgSO_4$, 4 mM Na_2HPO_4, and 100 mM HEPES, pH 7.4). The ghost suspensions were then incubated at 37 °C for 1 h. Erythrocyte ghosts prepared in the presence of millimolar Mg^{2+} have been shown to maintain normal lipid asymmetry and shape (Tanaka & Ohnishi, 1976; Williamson et al., 1985).

Preparation of Buds. Erythrocytes were incubated with A23187 (Calbiochem Corp., final concentration 0.01 mM) and Ca^{2+} (final concentration 0.2 mM) in 20 mM HEPES/145 mM NaCl, pH 7.4 at 37 °C, for 1 h. Membrane buds were isolated by centrifugation of supernatants at 30000*g* for 30 min. Any copelleted ghosts were removed by further centrifugation through a 20% (w/v) sucrose cushion, followed by washing with isotonic buffer. Lipid concentrations were determined by phosphate (Bartlett, 1959) and cholesterol (Zlatkis et al., 1953) assays.

Transfer across a Dialysis Membrane. A Spectropor dialysis membrane (Spectrum Medical Industries) with 500 000 molecular weight cutoff was washed and inserted into a microdialysis cell with two chambers and sideports (Belart Products). Water or sonicated vesicles (in NaCl/P_i) were added to chambers apposing cell suspensions, and incubations were carried out at room temperature. Transfer of hemoglobin was determined spectroscopically by measuring absorbances at 412 nm in the compartments. Transfer of lipid across the membrane was monitored by morphology changes in the cell compartment.

Transfer of Lipid from Vesicles. Acceptor membranes (cells or buds) were incubated with sonicated vesicles at the temperatures, concentrations, and time intervals specified in the text and figure legends. Cells and buds were separated from supernatant vesicles by layering aliquots of the suspensions on a sucrose cushion [42% (w/v) for cells, 20% (w/v) for buds] prepared in the appropriate buffer, and centrifuging at 13600*g* for 1 min for cells and at 35000*g* for 8 min for buds.

Transfer of Lipid from Cells. Erythrocytes loaded with transferrable lipid as above were incubated with acceptor membranes [resealed ghosts or DOPC/DPPG (97:3 mol/mol) sonicated vesicles]. Aliquots of incubation mixtures were removed and fixed for morphological analysis, or were centrifuged and the supernatants assayed for radioactivity.

EPR Spectroscopy. EPR spectra of spin PC incorporated cells and vesicles were taken in glass micropipets at room temperature, 9.15 GHz, and 100 mW with a Varian E-112 spectrometer.

Fusion Assay by NMR Spectroscopy. Erythrocytes in pH 5.5 buffer were mixed with Mn^{2+}-containing DMPC vesicles in a 10-mm NMR tube. ^{31}P-NMR spectra of the cell–vesicle suspension were recorded at 202.45 MHz on a General Electric GN-500 NMR spectrometer using a standard one-pulse sequence (90° excitation pulse, spectral width of 6500 Hz) without proton decoupling. All spectra were obtained at 37 °C.

[1] Abbreviations: DLPC, dilauroylphosphatidylcholine; DMPC, dimyristoylphosphatidylcholine; DOPC, dioleoylphosphatidylcholine; DPPC, dipalmitoylphosphatidylcholine; PC, phosphatidylcholine; lyso-PPC, lysopalmitoylphosphatidylcholine; DPPG, dipalmitoylphosphatidylglycerol; BSA, bovine serum albumin; spin PC, 1-palmitoyl-2-[9-(4,4-dimethyl-*N*-oxyoxazolidin-2-yl)stearoyl]phosphatidylcholine; SDS, sodium dodecyl sulfate; DIDS, 4,4′-diisothiocyano-2,2′-stilbenedisulfonic acid; HEPES, *N*-(2-hydroxyethyl)piperazine-*N*′-2-ethanesulfonic acid; MES; 2-(*N*-morpholino)ethanesulfonic acid; 2,3-DPG, 2,3-diphosphoglycerate; EPR, electron paramagnetic resonance; NMR, nuclear magnetic resonance; HCT, hematocrit; MI, morphological index.

Extraction of Incorporated Lipid. Cells (25% HCT) were incubated with DLPC vesicles (60 μM) at 37 °C for 30 min and then washed with buffer to remove any unincorporated vesicles. Cells were resuspended to 5% HCT in 1.25% (w/v) BSA and incubated for 30 min at 25 or 37 °C. In brief BSA treatments, cells (5% HCT) were washed twice with 1.25% (w/v) BSA at 4 °C. Cells were separated by centrifugation, washed once with buffer, and assayed for radioactivity.

DIDS Treatment. Erythrocytes were treated with 10 μM DIDS in $NaCl/P_i$ at 37 °C for 1 h, washed thoroughly with $NaCl/P_i$, and used immediately.

Enzyme Treatment of Cells. Erythrocytes were incubated in the presence of 25 μg/mL Pronase at 25% HCT for 30 min at 37 °C. Proteolysis was stopped by the addition of 0.25 mg/mL phenylmethanesulfonyl fluoride. Cells were then washed 3 times in $NaCl/P_i$ containing 15 mM EDTA. Sialic acid residues were removed by incubating cells with 0.1 unit/mL neuraminidase at 10% HCT for 90 min at 37 °C.

Scintillation Counting. Cell samples containing radioisotopes were bleached in 10 volumes of 30% H_2O_2 for 6–12 h at 60–80 °C. One volume of 10 mM NaN_3 was added prior to H_2O_2 as an antifoaming agent. Bleached samples were suspended in EcoLite (ICN Biomedicals, Inc.) and quantified with a scintillation counter (Model LS-3801; Beckman Instruments, Inc.). Counts were corrected to disintegrations per minute with a standard quench curve.

Cell Morphology. Erythrocytes were fixed in glutaraldehyde (0.5% in the buffer used in the lipid transfer incubation) for at least 10 min at room temperature. Samples were analyzed by light microscopy. Echinocytes were assigned scores of +1 to +5, with increasing values denoting more severe crenation; discocytes were scored 0; and stomatocytes were given scores of −1 to −4 (Bessis, 1973; Ferrell et al., 1985a; Daleke & Huestis, 1985). The average score of a field of 100 cells was defined as the morphological index (MI). Values shown in figures represent results of three replicate experiments, counted 3 times. Where absent in figures, error bars were smaller than the symbol size.

RESULTS

pH Dependence of Phospholipid Transfer

The pH dependence of DMPC transfer from sonicated vesicles to erythrocytes was examined using radiolabeled vesicles. As shown in Figure 1a, DMPC uptake by cells was accelerated at pH 5.5. These kinetic data were fit to the equation $y = a_0 + a_1[1 - \exp(-a_2 t)]$ by a nonlinear least-squares analysis. Initial rates and half-times were taken from the fitted curves and plotted as a function of pH (Figure 2). DMPC transfer at pH 5.5 was 3-fold (27 °C) or 4-fold (37 °C) faster than at pH 7.4. In contrast, a pH increase above pH 7.4 had little effect on DMPC transfer rates (Figure 2). No detectable extraction of cell cholesterol occurred in cell–vesicle incubations of this duration (data not shown).

DPPC transfer also was found to be accelerated at lower pH, although the cells rapidly lost 50% of associated DPPC to the supernatant when they were washed and treated with BSA (Figure 1b). On the supposition that the stably associated label reflected true lipid transfer, the initial rate of transfer was calculated to increase by a factor of 3.5 by changing the pH from 7.4 to 5.5. DOPC transfer also showed a similar acceleration at pH 5.5 (data not shown). In contrast, transfer of DLPC to cells was not altered by low pH (Figure 1c), and DMPC transfer was similarly insensitive at very low vesicle concentrations (inset, Figure 1a).

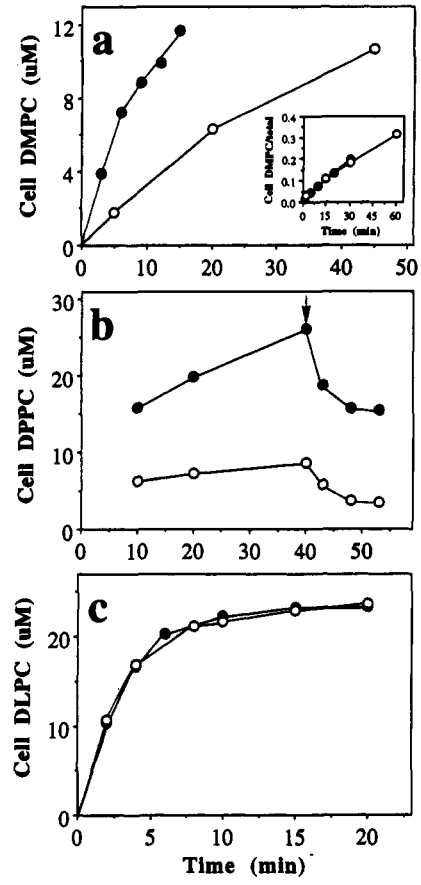

FIGURE 1: Effect of pH on transfer of phospholipid from vesicles to cells monitored by radiolabeled lipids. Transfer as a function of time of (a) DMPC for erythrocytes incubated at 37 °C with 72 or 0.14 μmol (inset) of DMPC/L of supernatant at 25% HCT, (b) DPPC from vesicles (125.3 μmol/L of supernatant) to cells (25% HCT) at 37 °C, and (c) DLPC from vesicles (25 μmol/L of supernatant) to cells (25% HCT) at 25 °C at pH 5.5 (●) and pH 7.4 (○). After the 40-min incubation of cells with DPPC vesicles (indicated by the arrow), aliquots of the cells were centrifuged and washed once with 20 volumes of $NaCl/P_i$, followed by incubation with BSA [final concentration 1.25% (w/v)] twice at 5% HCT for 5 min at 37 °C.

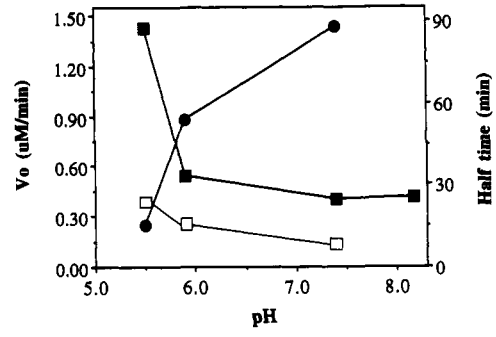

FIGURE 2: pH dependence of the initial rate of DMPC transfer from vesicles (73.6 μmol/L of supernatant) to cells (25% HCT) at 37 (■) and 27 °C (□), and the half-time at 37 °C (●).

On the other hand, lipid mixing between DMPC and spin PC vesicles measured by EPR spectroscopy did not show pH-induced acceleration from pH 7.4 to pH 5.5 at both low (2 mM) and high (13.33 mM) lipid concentrations (data not shown).

Possible Mechanisms of DMPC Transfer at Low pH

The pH dependence of lipid transfer might be explained by several processes that could be favored by lowering the cell pH. These mechanisms were tested using DMPC as the transferring lipid.

Table I: Assay for Cell–Vesicle Fusion by ^{31}P-NMR Spectroscopy

(A) Line-Width Change in A23187-Treated Cells[a] in Presence of Mn^{2+}

	2,3-DPG line width (Hz)	
$[Mn^{2+}]^b$ (μM)	3P	2P
0	67	60
5	80	84
10	119	129
20	nd[c]	nd[c]

(B) Line-Width Change during DMPC Transfer Incubation[d]

	2,3-DPG line width (Hz)	
time (min)	3P	2P
5	70	68
25	72	77
A23187	nd	nd

[a] 18 μM A23187 was added to cells at 60% HCT at pH 5.5. [b] Mn^{2+} was added from a 6.25 mM Mn^{2+}/3 mM Mg^{2+} stock solution. [c] Not detectable. [d] Cells at pH 5.5, 60% HCT, were incubated 37 °C with 0.64 mM DMPC vesicles containing 256 μM Mn^{2+} (encapsulated concentration).

Fusion at Low pH. Although spontaneous fusion between vesicles and the plasma membrane is an unusual event in the absence of fusogens (Rand & Parsegian, 1986), low pH might induce cell–vesicle fusion with concomitant lipid uptake at an apparently faster rate. Since the most rigorous criterion for fusion is the coalescence of the internal compartments of membranes, an NMR technique was used to detect mixing of cell and vesicle aqueous compartments (Sen and Huestis, unpublished results). Mn^{2+} was encapsulated in vesicles, excluded ions were removed by ion exchange, and vesicles were incubated with cells at pH 5.5. After 5 and 25 min at 37 °C, the ^{31}P-NMR spectrum of the sample was examined. Cell–vesicle fusion with pooling of aqueous contents would introduce Mn^{2+} into the cytosol, with concomitant interaction of Mn^{2+} with 2,3-DPG and consequent broadening of the metabolite's ^{31}P-NMR signals. Table IB shows the observed line widths of the 2- and 3-DPG phosphate resonances in cells exposed to Mn^{2+}-containing vesicles at pH 5.5. For comparison, 2,3-DPG line widths are shown for cells exposed to Mn^{2+} in the presence of the ionophore A23187 (Table IA). Samples containing vesicle-encapsulated Mn^{2+} showed no significant line broadening within 25 min. Samples containing the ionophore A23187 showed readily detectable line broadening when exposed to 5 μM Mn^{2+}, a concentration that would be delivered to the cytosol if 2% of the vesicles fused. Considering that at least 10% of the vesicle lipid was transferred to the cells, these results indicate that most of the transfer was not mediated by membrane fusion. Further, DMPC transfer at pH 5.5 was unaltered when vesicles were supplemented with 3% DPPG, an acidic phospholipid that inhibits PC vesicle fusion.

Adherence of Intact Vesicles to Cells at Low pH. Artifacts arising from adhesion of intact vesicles to cells could account for more rapid lipid uptake at low pH. This possibility was examined using rapid BSA washes at 4 °C. About 90% of DMPC transferred to cells at pH 5.5 as well as at pH 7.4 was not extractable by brief treatment with BSA. As a second test, cells incubated with spin PC vesicles (pH 5.5) were separated from supernatants, and the mode of binding was examined by EPR spectroscopy. The cells showed a high anisotropic triplet spectrum [see Figure 2c in Ferrell et al. (1985a)], indicating the insertion of spin PC into the cell membrane. The cell-associated spin PC was resistant to brief treatment with the reducing agent ascorbic acid. On the other hand, at both pH 5.5 and pH 7.4, 70–80% of the more soluble homolog DLPC was extracted from cells in extended BSA incubations at 25 or 37 °C, reflecting its outer monolayer intercalation. The amount of DLPC extracted by BSA from cells increased with increasing BSA concentration and time of incubation.

Cell Alterations at Low pH. (*a*) *Cell Shape.* Erythrocytes washed with pH 5.5 buffer become slightly cupped (MI = –0.75) at room temperature. Upon warming to 37 °C, these cells undergo a irreversible shape transformation which involves bleb formation and severe stomatocytosis (Lelkes & Fodor, 1991; Yang and Huestis, unpublished results). To examine the role of this shape change on lipid transfer, cells at pH 5.5 were fixed in 0.14% glutaraldehyde for 10 min at room temperature. This minimal fixation prevented the anomalous shape transformation at 37 °C, but the fixed cells took up DMPC at the same accelerated rate as pH 5.5 controls (data not shown). The effect of cell shape on lipid transfer also was examined using stomatocytes generated by chlorpromazine treatment. Chlorpromazine-treated and control cells incubated with DMPC vesicles gave similar lipid transfer rates (data not shown).

(*b*) *Cytosolic pH.* Low pH induces reorganization of membrane components (Elgsaeter et al., 1976; Arvinte et al., 1989a,b) and increases oxidative sensitivity, which might affect uptake of foreign lipid. Oxidative damage initiated by hemoglobin oxidation at low pH was inhibited by CO treatment, and DMPC uptake was examined. The lipid transferred to carboxygenated and control cells at almost identical rates (data not shown). In addition, cells were pretreated with the anion transport inhibitor DIDS (Cabantchik & Rothstein, 1974) to inhibit cytosolic pH change. These cells were washed with pH 5.5 buffer and incubated at pH 5.5 for 60 min at 37 °C. After the incubation, the intracellular pH was 7.01, as determined by freeze–thaw lysis of packed cells. DMPC transfer to these cells at pH 5.5 was as rapid as to DIDS-free controls (data not shown).

While these results demonstrated that the pH of the suspending medium is the factor that alters lipid transfer rates, they provided no clear physical basis for the acceleration found at low pH. Further experiments addressed the possibility that the transfer mechanism changes with pH through alterations in intermembrane interactions.

Effect of Donor–Acceptor Membrane Proximity

Transfer across a Dialysis Membrane. In a pure monomer transfer process where monomer desorption from the donor is rate-limiting, the rate should not be affected by the distance between donor and acceptor membranes. PC transfer from vesicles to cells through an intervening dialysis membrane was examined. Transfer of water across the dialysis membrane to the cell compartment was rapid (within 5 min), and the resulting free hemoglobin passed through the membrane at a readily detectable rate (Figure 3a). DLPC transfer across a membrane was, however, undetectable in 5 h, while transfer without an intervening membrane occurred in 10 min (Figure 3b). Increased DLPC (0.5 mM) in the vesicle compartment did not increase the transfer rate. In contrast, more soluble lipids showed passage through the dialysis membrane (Figure 3c) slowly (lyso-PPC) or fairly rapidly (SDS), in agreement with an earlier report on lysolipid transfer (Weltzien, 1979).

Effect of Sample Volume on Transfer Kinetics. The role of donor-to-recipient membrane close approach was examined in studies of DLPC and lyso-PPC transfer between intact

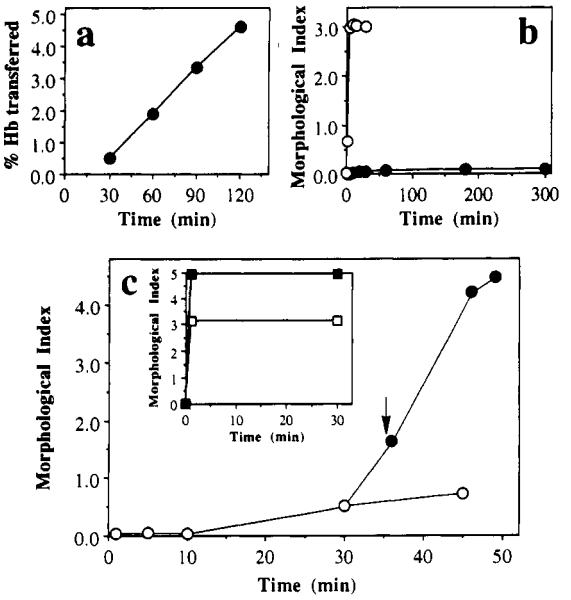

FIGURE 3: Transfer of lipid across a dialysis membrane at 23 °C monitored by cell morphology. (a) Hemoglobin transfer after lysis by H_2O passed through a membrane (cells 27% HCT). (b) DLPC transfer from vesicles (69 μmol/L of supernatant) to cells (27% HCT) across (●) and without (○) a dialysis membrane. (c) Transfer of lyso-PPC from vesicles (50 μmol/L of supernatant) to cells (50% HCT) across a membrane (○). At 35 min (arrow), 0.5% (w/v) SDS was added to the vesicle compartment, and the morphology change was monitored (●). The inset shows lyso-PPC (□) and SDS (■) transfer without a membrane.

cells and resealed ghosts. Transfer was monitored from changes in the morphology of the donor cells, a parameter that correlates reliably with foreign lipid content in the membrane outer monolayer (Ferrell et al., 1985a; Daleke & Huestis, 1985, 1989). This rapid and sensitive method yields kinetic results that are quantitatively consistent with values determined from radiolabel transfer (see below).

Intact cells were first incubated with DLPC vesicles (1 volume, 150 μM) or lyso-PPC micelles (1 volume, 200 μM) until samples reached a steady-state echinocytic morphology. Unincorporated lipid was removed from DLPC samples, and the resulting echinocytes (stages 3–4) were resuspended with resealed ghosts (with an echinocyte:ghost ratio of 1:12 in all samples) in varying volumes of NaCl/P_i. Samples were incubated at 23 °C, and the morphologies of the intact cells (which are readily distinguished from ghosts in microscopic fields) were monitored. As the transferrable lipid equilibrated between intact cells and the excess ghost membranes, the MI of the echinocytes fell, and the cells became discoid (Figure 4a). Intact echinocytes incubated for over 5 h under identical conditions in the absence of recipient ghosts retained stable spiculate shape (data not shown). Thus, the morphology change in cells incubated with ghosts reflects loss of transferrable lipid from the cell outer monolayer to the ghost membrane sink.

Transfer of DLPC from cells to ghosts showed a significant dependence on the volume of the suspension. At a constant donor-to-acceptor ratio, the morphology change of donor cells slowed dramatically as cell and ghost concentrations were diluted: 5-fold dilution produced a greater than 6-fold decrease in the rate of DLPC transfer (Figure 4a). In contrast, lyso-PPC transfer kinetics (Figure 4b) were not affected detectably by a 100-fold change in cell and ghost concentrations (again measured at a constant cell:ghost ratio). Lyso-PPC transfer was too rapid to permit accurate estimation of initial rates, but equilibration between intact cells and ghosts appeared

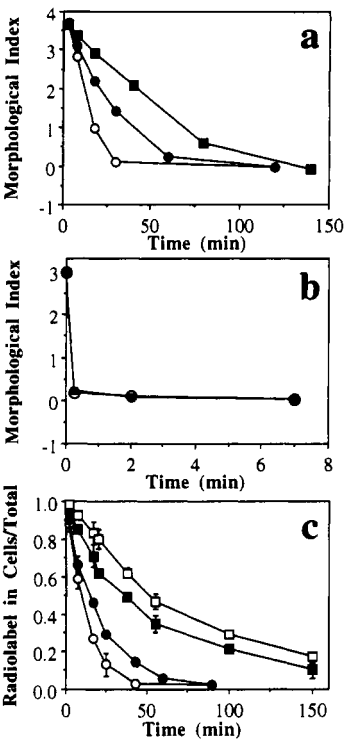

FIGURE 4: Effect of aqueous volume on lipid transfer at 23 °C from cells to ghosts monitored by cell morphology. (a) DLPC transfer for 8.33% cells (○), 2.78% cells (●), and 1.64% cells (■) at a constant cell-to-ghost ratio of 1:12. (b) Lyso-PPC transfer for 8.33% cells (○) and 0.06% cells (■) at a constant cell-to-ghost ratio of 1:12. (c) DLPC transfer from cells to ghosts (at constant cell-to-ghost ratio of 1:47.5) as monitored by [^{14}C]DLPC. Data are for cells at 1.5% HCT (○), 0.75% HCT (●), 0.375% HCT (■), and 0.15% HCT (□).

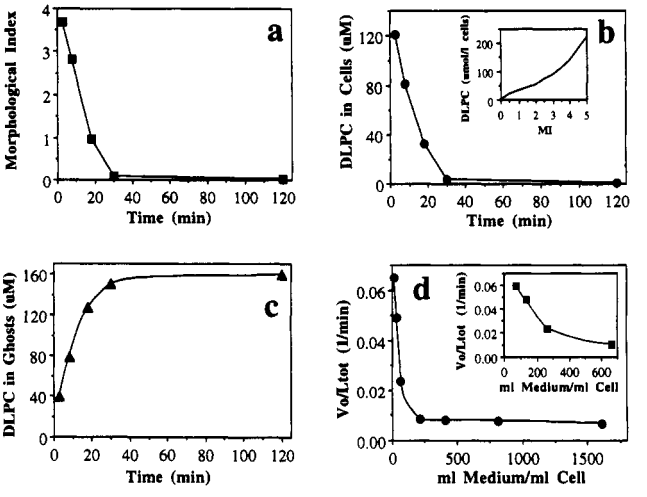

FIGURE 5: Transfer of DLPC from cells to ghosts at 23 °C. (a) Cell morphology as a function of time for DLPC-loaded erythrocytes (8.33% HCT) incubated with ghosts (100% HCT). (b) DLPC remaining in cells, calculated from the relationship between DLPC incorporation and morphology (inset). (c) DLPC transferred to ghosts, calculated from (b). (d) Initial rate of DLPC transfer as a function of the aqueous volume at a constant cell-to-ghost ratio of 1:12. In the inset, the initial rate of DLPC transfer calculated from Figure 4c is plotted as a function of the aqueous volume at a constant cell-to-ghost ratio of 1:47.5.

complete for both dilute and concentrated samples at the earliest measurable point.

DLPC remaining in the intact cells at a given time was estimated from the relationship between cell morphology and lipid incorporation [Figure 5a,b; as described in Ferrell et al. (1985a,b)]. DLPC transferred to ghosts also was calculated

and plotted (Figure 5c) to obtain initial rates of transfer. When the initial rates obtained from the fitted curves as described above were plotted as a function of the aqueous volume (Figure 5d), the initial rate decreased with increasing volume (decreasing donor and acceptor concentrations), eventually reaching a volume-insensitive plateau.

The results of these morphology-based studies were verified by direct measurement of [^{14}C]DLPC transfer from cells to ghosts. Erythrocytes prelabeled with [^{14}C]DLPC were incubated with a 47.5-fold excess of resealed ghosts in varying volumes of buffer. At times designated in Figure 4c, aliquots of cells were isolated, and residual radiolabel was quantified. The rate of [^{14}C]DLPC loss was inversely proportional to volume (inset, Figure 5d), quantitatively consistent with results obtained using cell morphology changes.

The indistinguishably rapid transfer of lyso-PPC at widely differing membrane concentrations is consistent with monomer transfer through the aqueous phase, with monomer dissociation from the donor as the rate-limiting event. In contrast, variation of transfer kinetics with cell/ghost concentrations suggests that DLPC transfer is mediated in part by donor and acceptor membrane encounter.

Development of the Kinetic Model. A model that accounts for the observed DLPC transfer kinetics must include both monomer passage through the aqueous phase and close approach of the donor and acceptor membranes. Simple monomer transfer is a two-step process, with the dissociation of a monomer from the donor membrane as the rate-determining step. The monomer then diffuses through the aqueous phase and is incorporated into the acceptor membrane. The derivation of an expression for this process is presented by Ferrell et al. (1985a). The rate of lipid transfer is described by

$$\frac{dL_d}{dt} = \frac{d[L_d - (L_d)_{eq}]}{dt} = -k_{app}[L_d - (L_d)_{eq}] \quad (1)$$

with an apparent rate coefficient

$$k_{app} = \frac{k_1k_{-2} + k_1k_2A + k_{-1}k_{-2}D}{k_{-2} + k_{-1}D + k_2A} \quad (2)$$

where D and A represent the donor and acceptor membrane concentrations, respectively, L_d is the concentration of transferrable lipid in the donor membrane, and $(L_d)_{eq}$ is the equilibrium concentration of L_d. k_1 and k_{-2} are dissociation rate coefficients from the donor and acceptor membranes, respectively, and k_{-1} and k_2 are association rate constants for the donor and acceptor membranes, respectively. Integration of eq 1 yields

$$[L_d - (L_d)_{eq}]_t = [L_d - (L_d)_{eq}]_0 \exp(-k_{app}t) \quad (3)$$

where $(L_d)_0$ is the initial concentration of transferrable lipid in the donor membranes. To simplify the calculation, $[L_d - (L_d)_{eq}]_t/[L_d - (L_d)_{eq}]_0$ is converted to $1 - (L_a)_t/(L_a)_{eq}$ where $(L_a)_t$ is the concentration of lipid transferred to the acceptor membrane at time t and $(L_a)_{eq}$ the equilibrium concentration of lipid transferred.

When the donor membranes are cells and the acceptor membranes are cells or resealed ghosts, dissociation and association rate coefficients for the donor and acceptor membranes can be assumed to be approximately equal, respectively; $k_1 = k_{-2}$ and $k_{-1} = k_2$. This simplification yields $k_{app} = k_1$.

If lipid molecules also may transfer in a transiently apposed complex of the donor and acceptor membranes, an additional term should be incorporated into the rate expression. This leads to the integrated form

$$[L_d - (L_d)_{eq}]_t = [L_d - (L_d)_{eq}]_0 \exp\{-(k_1 + k_cA)t\} \quad (4)$$

where k_c is the rate coefficient for transfer in the transient complex. Therefore, a plot of –slope, which is obtained from a semilog plot of transfer vs time, against A yields an intercept of k_1 and a slope of k_c.

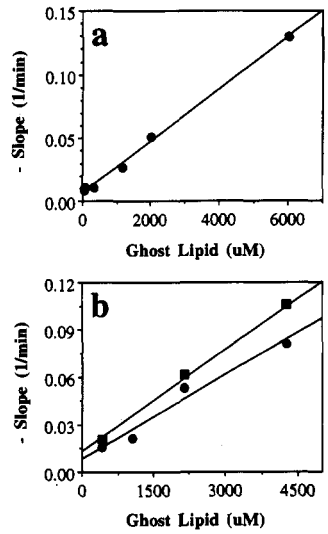

FIGURE 6: Plots of the slope of log transfer of DLPC vs time against ghost lipid concentration. (a) Data are from Figure 5. (b) DLPC transfer from cells to ghosts at a constant cell-to-ghost ratio of 1:47.5 at 23 °C was monitored by [^{14}C]DLPC. Circles are for pH 7.4 and squares for pH 5.5.

On the other hand, when donor and acceptor membranes differ in composition and geometry, dissociation rates may not be equivalent, and the simplification of eq 2 may be invalid. In these systems, an initial rate approximation permits simplification of the model. The differential equation for the initial rate between the donor and acceptor membranes (Jones & Thompson, 1989) is

$$\frac{dL_d}{dt} = \frac{k_1k_{-1}DL_d}{k_{-1}D + k_2A} - k_1L_d - k_cAL_d = -(k_m + k_cA)L_d \quad (5)$$

with a rate coefficient for monomer transfer, $k_m = k_1k_2A/(k_{-1}D + k_2A)$, and a rate coefficient for transient collision transfer, k_c. Again, the plot of –slope against A yields a slope of k_c and an intercept of k_m, not k_1; k_m can be approximated to k_1 only when $k_{-1}D \ll k_2A$.

Transfer of DLPC from Cells to Ghosts. Data for DLPC transfer from cells to ghosts were fitted as described above. Slopes were obtained from a semilog plot of transfer vs time. A plot of the negative values of these slopes vs the ghost lipid concentration [calculated on the basis of the fact that 1% cell suspension has the same membrane surface area as a 60.12 μM suspension of vesicles (Ferrell et al., 1985b)] yielded a straight line with a k_1 of 7.19×10^{-3} min^{-1} and a k_c of 1.80×10^{-5} μM^{-1} min^{-1} (Figure 6a).

Data from radiolabel transfer experiments were analyzed similarly. Semilog plots of transfer vs time yielded straight lines, and –slopes of those lines were plotted as a function of the lipid concentration of ghosts (Figure 6b). The slope of the plot in Figure 6b gave a k_c of 1.79×10^{-5} μM^{-1} min^{-1} with an intercept, k_1, of 7.39×10^{-3} min^{-1} at pH 7.4. These values were closely similar to those obtained from morphology changes, verifying the validity of the more convenient morphology-based assay. Similar analysis of transfer data obtained at pH 5.5 yielded a k_1 of 9.02×10^{-3} min^{-1} and a

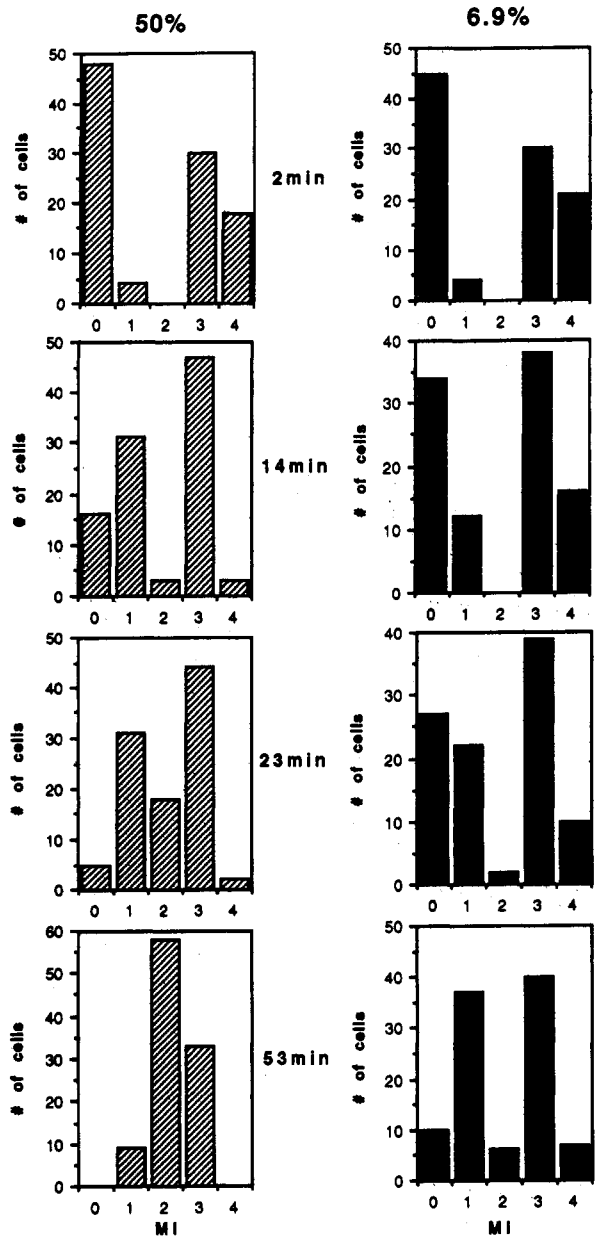

FIGURE 7: Transfer of DLPC between cells at 23 °C. Erythrocytes incubated with DLPC were mixed with an equal volume of normal discocytes at 50% HCT (left) and 6.9% HCT (right). At the time points indicated, aliquots were removed and fixed, and the number of cells at each morphological stage was tabulated.

k_c of 2.34×10^{-5} μM^{-1} min^{-1}, values slightly higher than found at pH 7.4.

Cell-to-Cell Transfer of DLPC. Erythrocytes were incubated with DLPC vesicles to yield echinocytes, and these cells were reincubated with an equal volume of untreated discocytes at 23 °C. Initially, these samples contained two distinct populations of cells (Figure 7). At 50% combined HCT, these populations merged to generate a single population of intermediate-stage echinocytes within 53 min. Dilution of the cell suspension, however, slowed down this process; at 6.9% combined HCT, the cell suspension retained bimodal shape distribution after 53 min (Figure 7).

The rate at which the cell populations converged was analyzed to obtain rates of cell-to-cell lipid transfer. MIs were calculated for the 50% cells with lower MIs (the acceptor population), and these were plotted as a function of time, as the initially discoid cells became echinocytic. The results of one such analysis are shown in Figure 8a. The morphological

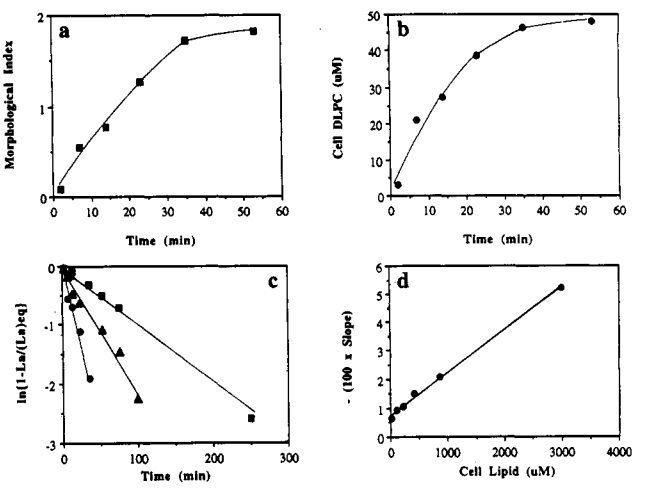

FIGURE 8: Cell-to-cell transfer of DLPC at 23 °C. (a) Morphology of 50% cells with lower MIs (acceptor population) as a function of time at 50% HCT. (b) DLPC transferred to discocytes, calculated from the relationship between lipid incorporation and morphology. (c) log transfer as a function of time at 50% HCT (●), 14.3% HCT (▲), and 3.7% HCT (■). (d) A graph of the slope obtained from (c) as a function of cell lipid concentration.

index was then converted to lipid concentration (Figure 8b), and plots of log of transferred lipid (transfer) vs time (Figure 8c) yielded straight lines whose slopes decreased with decreasing cell concentrations. A plot of –slope vs cell concentration (Figure 8d) yielded a k_1 of 9.21×10^{-3} min^{-1} and a k_c of 1.43×10^{-5} μM^{-1} min^{-1}, values close to those obtained for cell-to-ghost transfer.

Transfer of DLPC from Cells to DOPC Vesicles. Cells labeled with DLPC plus [^{14}C]DLPC (MI = +1.5) were washed once and incubated at 23 °C, pH 7.4, with a constant ratio of excess vesicles composed of DOPC plus 3% (mol/mol) DPPG. Under the conditions employed, DOPC was nontransferrable. At a constant ratio of donor-to-acceptor membranes (1:47.5), the initial rate of DLPC transfer to DOPC vesicles increased with increasing cell and vesicle concentrations (Figure 9a,b). From plots in Figure 9c, values of k_1 ($=k_m$ because $k_2A \gg k_{-1}D$) and k_c were calculated to be 9.77×10^{-3} min^{-1} and 4.63×10^{-5} μM^{-1} min^{-1}, respectively. The former coefficient was very similar to values obtained for transfer from cells to cells or ghosts, but the latter, the rate coefficient for transient collision transfer, was 3.5-fold larger for vesicles than for cells and ghosts at the same donor and acceptor concentrations.

Transfer of Lyso-PPC and DLPC from Cells to Water. Cells were incubated with lyso-PPC or DLPC vesicles to yield stage 3 echinocytes. These cells were diluted into varying volumes with NaCl/P_i at 23 °C. The critical bilayer concentration of lipid from cells was determined as follows. The rate of dissociation of lipid molecules from cells is expressed as

$$dL_c/dt = -k_d L_c + k_a L_m C \quad (6)$$

where, again, C is the cell lipid concentration, L_c is the concentration of cell-bound foreign lipid, L_m is the concentration of free monomers, and k_d and k_a are the dissociation and association rate coefficients, respectively. At equilibrium, the apparent rate of dissociation is 0, and thus $k_d L_c$ equals $k_a L_m C$. The critical bilayer concentration (cbc), defined as k_d/k_a, is expressed as

$$\text{cbc} = k_d/k_a = L_m C/L_c \quad (7)$$

Thus, L_m and L_c were determined from the final MIs of diluted

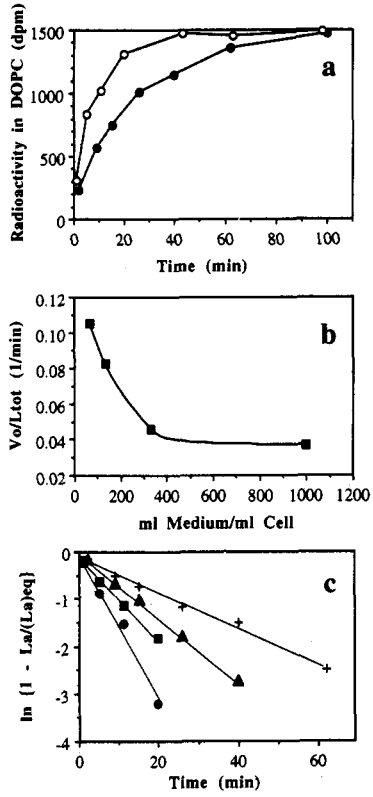

FIGURE 9: Transfer of DLPC from cells to DOPC vesicles at a constant cell-to-vesicle ratio of 1:47.5 at 23 °C. (a) [^{14}C]DLPC appearance in DOPC vesicles at 4.3 (○) and 0.287 mM (●) as a function of time. (b) Initial rate of DLPC transfer as a function of the aqueous volume. (c) log transfer as a function of time at 4.3 (●), 2.15 (■), 0.86 (▲), and 0.287 mM (+).

cell samples (for lyso-PPC at 0.0078–50% HCT), or by using radiolabeled lipid (for DLPC at 0.005–0.015% HCT). Critical bilayer concentrations obtained from plots of L_m/L_c vs $1/C$ were 0.34 and 6.44 μM for DLPC and lyso-PPC, respectively. These values are very similar to their critical micelle concentrations [0.36 μM for DLPC interpolated from the data summarized in Tanford (1980), and 7 μM for lyso-PPC reported by Haberland and Reynolds (1975)].

At early times, the concentration of free monomers can be set to 0. Thus, the second term in eq 6 can be ignored, and the integration of the equation yields

$$(L_c)_t = (L_c)_0 \exp(-k_d t) \quad (8)$$

Therefore, dissociation rate coefficients from cells were obtained from semilog plots of lipid loss vs time. The dissociation rate coefficients determined from triplicate data at 0.005% and 0.0025% HCT for DLPC, and from duplicate data at 0.31%, 0.16%, and 0.078% for lyso-PPC, were (8.25 ± 1.46) × 10^{-3} min^{-1} and (1.17 ± 0.58) × 10^{-1} min^{-1}, respectively. These values showed an acyl chain dependence similar to the cbc's; the former was 14-fold lower and the latter 19-fold lower for DLPC than for lyso-PPC.

Transfer of DLPC from DLPC Vesicles to Cells. Erythrocytes were incubated (23 °C) with DLPC vesicles at two membrane concentrations: 50% HCT cells with 60 μM DLPC and 2.5% HCT cells with 3 μM DLPC. Initial rates of transfer were not significantly different in the two samples; the rate (v_0/L_{tot}) was 0.276 min^{-1} for the high HCT and 0.255 min^{-1} for the low HCT. This result was consistent with simple monomer transfer. The monomer dissociation rate coefficient determined from a double-reciprocal plot of $1/v_0$ vs $1/C$ (Ferrell et al., 1985b) was 0.318 min^{-1}. No values for transfer

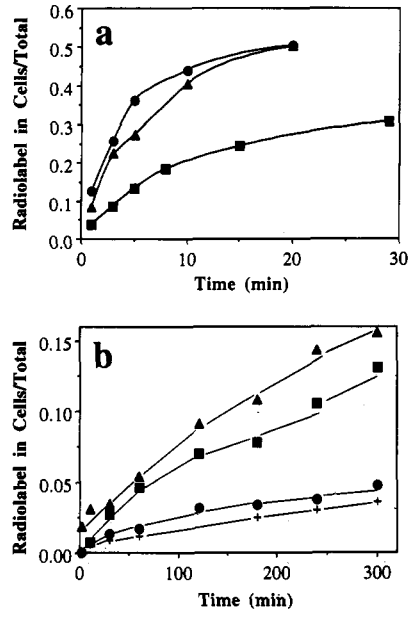

FIGURE 10: Transfer of lipid from DOPC/3% DPPG vesicles to cells at 23 °C. (a) DLPC transfer at a constant DOPC-to-cell ratio of 1:1 at 50% HCT (●), 25% HCT (▲), and 5% HCT (■). (b) DMPC transfer at a constant DOPC-to-cell ratio of 1:1 at 50% HCT (▲), 25% HCT (■), 5% HCT (●), and 2.5% HCT (+).

in collisional complexes can be obtained from these data because the donor vesicle concentration rapidly approaches zero; thus, the model is not valid for this experiment.

Transfer of DLPC and DMPC from DOPC Vesicles to Cells. In order to keep the donor membrane concentration constant throughout the lipid transfer incubation, inert DOPC vesicles containing 3% (mol/mol) DPPG were used as donors. DOPC vesicles cosonicated with DLPC plus [^{14}C]DLPC (DOPC:DLPC ratio = 127.5 mol:1 mol) or with DMPC plus [^{14}C]DMPC (DOPC:DMPC ratio = 84.8 mol:1 mol) were incubated with a constant ratio of erythrocytes in various volumes of NaCl/P$_i$ at 23 °C. Lipid transfer showed a volume dependence for DLPC as well as for DMPC (Figure 10). The values of k_m and k_c were then obtained from these data as described above: 2.45 × 10^{-2} min^{-1} and 3.47 × 10^{-5} μM^{-1} min^{-1} for DLPC; 2.43 × 10^{-4} min^{-1} and 3.15 × 10^{-7} μM^{-1} min^{-1} for DMPC. The monomer dissociation rate coefficients were determined as described (Ferrell et al., 1985b) at low cell concentrations: 9.24 × 10^{-2} min^{-1} for DLPC; 9.15 × 10^{-4} min^{-1} for DMPC. Thus, all the rate coefficients were about 100-fold greater for DLPC than for DMPC, indicating both monomer and transient collision rates are dependent on the acyl chain length.

pH Dependence of Lipid Transfer Kinetics. The pH dependence of DMPC transfer was analyzed according to the kinetic model developed above. Cells were incubated at pH 5.5 and 7.4 with a constant ratio of DMPC vesicles at 37 °C. Plots of −slope vs cell lipid concentration gave a slope 9-fold higher at pH 5.5 than at pH 7.4 (Figure 11a). k_1 values determined as described (Ferrell et al., 1985b) were closely similar for both pH values, while k_c was an order of magnitude greater at pH 5.5 (Table IV).

DMPC Transfer to Buds. The pH dependence of DMPC transfer to Ca^{2+} buds was studied at 37 °C. The values of k_m and k_c were obtained from intercepts and slopes of plots shown in Figure 11b. k_1 values obtained at low bud concentrations were again closely similar at the two pHs, while the k_c value was larger at pH 5.5. The increase in k_c at low pH was not as great for buds as when cells were used as acceptors (Table IV).

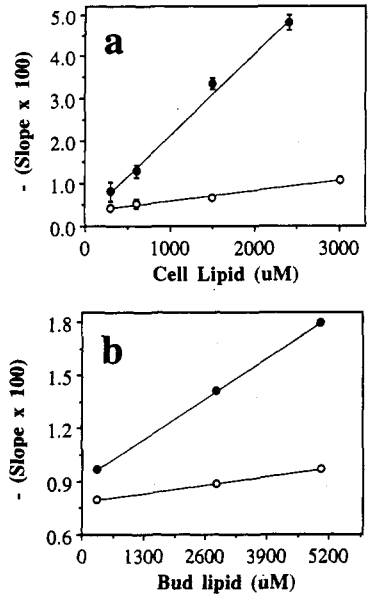

FIGURE 11: pH effect on DMPC transfer at 37 °C. (a) DMPC transfer to cells at a constant vesicle-to-cell ratio of 1:20, and (b) to buds at a constant vesicle-to-bud ratio of 1:30. Closed circles are for pH 5.5 and open ones for pH 7.4.

Effect of Removal of Glycosylated Components on the Cell Surface. Cells treated with neuraminidase have been reported to have 50–80% of the sialic acid removed, without accompanying proteolysis (Fairbanks et al., 1971; Gokhale & Metha, 1987; Othmane et al., 1990). Desialiated cells were incubated with DMPC vesicles at 37 °C, pH 7.4, and their DMPC uptake was compared to untreated cells. Desialiation resulted in a 1.5-fold increase in the initial rate of transfer, consistent with facilitated collisional events for the less charged acceptor membrane. This surface effect was also confirmed using cells treated with Pronase, which is reported to remove two-thirds of the total sugar on the cell surface (Garnier-Suillerot & Gattegno, 1988). DMPC transfer to Pronase-treated cells was 2-fold faster than to control cells.

DISCUSSION

Effects of alterations of the aqueous environment on spontaneous transfer of lipids have been demonstrated; ionic strength alters interbilayer transfer of zwitterionic as well as charged phospholipids (Papahadjopoulos et al., 1976; De Cuyper et al., 1983; Jones & Thompson, 1990), and pH alters phospholipid transfer (De Cuyper & Joniau, 1985; Gardam et al., 1989; Massey et al., 1982). However, little attention has been paid to pH effects on PC transfer, because it is expected to be inert to pH changes in biologically relevant ranges; the pK_a[2] of the phosphate is 2–3 (Boggs, 1980; Hauser & Phillips, 1979), and the quaternary ammonium is charged at all pH values. The present study was motivated by the observation that, contrary to this expectation, DMPC transfers from vesicles to cells 4-fold faster at pH 5.5 than at pH 7.4. The experiments detailed here examine the basis for this kinetic difference, employing a combination of radiolabel and cell morphology assays to measure PC transfer between membranes of varying sizes and configurations, at pH 5.5 and 7.4.

pH Dependence. The present study shows that while PC transfer rates are very similar at pH 7.4 and 8.17, DMPC, DPPC, and DOPC transfer from vesicles to cells much more rapidly at pH 5.5 (Figure 1). In contrast, the comparatively less hydrophobic homolog DLPC transfers at identical rates at all pH values examined. When DMPC transfer was examined further at pH 5.5, a deviation from saturable first-order kinetics was observed at high membrane concentrations, and k_1 [calculated on the basis of the model presented in Ferrell et al. (1985b)] was found to increase by a factor of 27.6 at 37 °C. These results are not predicted by a pure monomer transfer model: the solubility of DMPC should not be affected in this pH range (indeed, if the cmc of PC were pH-dependent, DLPC transfer should also accelerate at low pH). The half-time of DMPC exchange between vesicles is reported to be 2 h at pH 6 (McLean & Phillips, 1984a,b), similar to values obtained at pH 7.4. Massey et al. (1982) also reported no change in the half-time of fluorescent PC transfer between apolipoprotein–phospholipid recombinants from pH 5.5 to 10. Studies on lipid mixing in PC vesicles using fluorescent phosphatidylethanolamine (Massari et al., 1991) also showed only a slight increase (1.6-fold at 37 °C) in the lipid exchange rate even at pH 4.

Examination of possible mechanisms of DMPC transfer at pH 5.5 revealed that (a) fusion is not involved, (b) DMPC molecules are not simply loosely associated with the cells, but are intercalated into the outer monolayer of the membrane, (c) obvious cell responses (oxidative damage, morphology, cytosolic pH) to pH change do not affect lipid transfer rates, and (d) extracellular pH is the controlling variable.

Reconsideration of the Monomer Transfer Model. To gain more insight into the mechanism of lipid transfer, attempts were made to evaluate the extent to which monomer transfer controls intermembrane traffic at pH 7.4. DLPC was chosen for this study because it shows some characteristics of monomer transfer, as follows: (a) double-reciprocal plots ($1/v_0$ vs $1/C$ or $1/L_{tot}$) of the data in vesicle-to-cell transfer yield parallel lines (Ferrell et al., 1985b); (b) DLPC transfer from vesicles to cells is pH-independent (Figure 1c); and (c) intercell transfer is also pH-independent (data not shown).

Dialysis membrane experiments demonstrated that very soluble lipids transfer rapidly between separate compartments, consistent with monomer transfer. However, this experimental approach is not feasible for less soluble lipids, whose monomer concentration is too low to drive passage through a membrane. The effect of intermembrane distance on transfer of these lipids was examined by dilution experiments. According to Ferrell et al. (1985b), when phospholipids were used at concentrations greatly in excess of their critical bilayer concentrations, the initial rate of lipid transfer is given by

$$v_0/L_{tot} = \frac{k_1 k_2 A}{k_{-1} D + k_2 A} = \frac{k_1 k_2 A/D}{k_{-1} + k_2 A/D} \qquad (9)$$

where A represents the acceptor lipid concentration, L_{tot} the total lipid concentration, and D the donor lipid concentration. Thus, the monomer transfer model predicts that the actual concentrations of the donor and acceptor membranes should not affect the initial transfer rates as long as the ratio of donor to acceptor membranes (A/D) is kept constant. The present results are not consistent with this simple monomer transfer model; initial rates of DLPC transfer vary with the aqueous volume under many circumstances (cell-to-ghost, Figures 4a and 5d; cell-to-cell, Figure 7; cell-to-vesicle, Figure 9a,b; vesicle-to-cell, Figure 10a), although the volume dependence of transfer becomes insignificant for DLPC transfer from DLPC vesicles and for lyso-PPC transfer (cell-to-ghost, Figure

[2] This is the pK_a value for the pure phospholipid at the bilayer–water interface. The intrinsic pK_a of the phosphate group in DMPC and DPPC is lower than 1 (Träuble & Eibl, 1974). Note that the pK_as of ionizable groups in phospholipids are sensitive to their environment.

Table II: Summary of Rate Coefficients for DLPC Transfer[a]

donor	acceptor	k_1 (min^{-1})	k_c (μM^{-1} min^{-1})	k_c' (μM^{-1} min^{-1})[b]
DOPC	cell	9.24×10^{-2}	3.47×10^{-5}	6.94×10^{-5}
cell	DOPC	9.77×10^{-3}	4.63×10^{-5}	6.61×10^{-5}
cell	cell	9.21×10^{-3}	1.43×10^{-5}	2.86×10^{-5}
cell	ghost	7.39×10^{-3}	1.79×10^{-5}	3.58×10^{-5}
DLPC	cell	3.18×10^{-1}	*c*	*c*

[a] DLPC transfer incubations were carried out at pH 7.4 at 23 °C. [b] Rate coefficients were calculated in terms of outer monolayer lipid concentrations of acceptor membranes. [c] Not measurable.

Table III: Summary of Rate Coefficients for DMPC Transfer[a]

donor	acceptor	k_c (μM^{-1} min^{-1})	k_1/k_c (μM)
DMPC	cell	2.17×10^{-6}	3.37×10^{3}
DMPC	bud	3.63×10^{-7}	2.16×10^{4}
DMPC	DMPC	2.17×10^{-7} [b]	3.1×10^{4} [b]

[a] DMPC transfer incubation was carried out at pH 7.4 at 37 °C. [b] Reported by Jones and Thompson (1990) at 30 °C.

Table IV: Summary of pH Effects on Lipid Transfer Rate Coefficients

transferrable lipid	donor	acceptor	temp (°C)	pH	k_1 (min^{-1})	k_c (μM^{-1} min^{-1})
DLPC	cell	ghost	23	7.4	7.19×10^{-3} [a]	1.80×10^{-5} [a]
					7.39×10^{-3} [b]	1.79×10^{-5} [b]
DLPC	cell	ghost	23	5.5	9.02×10^{-3}	2.34×10^{-5}
DMPC	DMPC	cell	37	7.4	7.31×10^{-3}	2.17×10^{-6}
DMPC	DMPC	cell	37	5.5	7.17×10^{-3}	1.96×10^{-5}
DMPC	DMPC	bud	37	7.4	7.84×10^{-3}	3.63×10^{-7}
DMPC	DMPC	bud	37	5.5	9.15×10^{-3}	1.75×10^{-6}

[a] Rate coefficients determined by MI assays. [b] Rate coefficients determined using radiolabeled lipid.

4b). Note that in these latter cases, monomer desorption rates are relatively fast.

New Kinetic Model. The volume dependence manifested above provides strong kinetic evidence that the transfer involves a collisional event in addition to the monomer desorption process. A new model was developed based on Jones and Thompson's observations of a second-order concentration-dependent process for lipid exchange between PC vesicles (Jones & Thompson, 1989). As predicted by the new model, -slope obtained from a semilog plot of lipid transfer vs time was proportional to acceptor membrane concentration at a fixed donor-to-acceptor ratio (Figures 6a, 6b, and 8d for DLPC; Figure 11a,b for DMPC). Accordingly, the rate coefficients were calculated and summarized in Tables II, III, and IV.

From these results, several conclusions can be drawn regarding the mechanism of lipid transfer. First, the transient collision rate coefficient is proportional to the monomer transfer rate coefficient, which precludes a model in which the transient collision transfer occurs via a partially fused complex (Ferrell et al., 1985b; Gurd, 1960). This result instead suggests that monomer transfer is also involved in the transient collision process. Second, donor membrane configuration apparently affects which kinetic process predominates (Table II). For example, when DLPC transfer from DOPC vesicles to cells is compared with the reverse process (cell-to-DOPC vesicle transfer), the monomer transfer rate coefficient k_1 is an order of magnitude greater for the vesicle donor/cell recipient pair than for the reverse, while rate coefficients for collisional transfer are similar. This is consistent with reported effects of donor surface curvature (Fugler et al., 1985; McLean & Phillips, 1984a,b; Thomas & Poznansky, 1988), and further it suggests that collisional transfer is relatively more significant in the case of cell-to-vesicle transfer. Comparing transfer from cells to various recipients, monomer transfer rates are similar for cell, ghost, or vesicle acceptors, but collisional transfer is 3-fold more rapid for vesicle acceptors. Where the donor membrane is pure DLPC, the flux arising from the monomer transfer mechanism dominates, which makes the collision term relatively negligible. Third, the transient collision coefficient is dependent on the sizes of reacting membranes (Tables II and III). As summarized in Table III, transfer of DMPC from DMPC vesicles is an order of magnitude more rapid for a cell acceptor than for membrane buds or intervesicle exchange. k_1 values for the three systems are closely similar; the accelerated transfer reflects an increase in collisional transfer. The same effect is seen for DLPC transfer (Table II). A primary distinction between cells and vesicles as lipid acceptors is the difference in their curvature; a higher proportion of vesicle lipid is in the surface monolayer. When the transient collision coefficient is normalized to the outer monolayer lipid concentration of the acceptor membrane, similar values are obtained for DLPC transfer between DOPC vesicles and cells (Table II, k_c'). Similar normalization for the surface area indicates that cell–cell or cell–ghost collisional transfer is about 2-fold slower than transfer where one participant is a vesicle. This likely reflects steric and repulsive Coulombic interactions that are greatest where both participants are natural membranes. Also, because of the relatively large mass of cells, the frequency of cell–cell collisions would be small compared to cell–vesicle collisions. On the other hand, comparison of k_1/k_c values shows that the transient collision process is more efficient for vesicle-to-cell transfer than for vesicle-to-bud transfer, which is more efficient than for vesicle-to-vesicle transfer (Table III); larger acceptor targets collide more efficiently with donors. Also, cell membranes may have laterally segregated domains of low charge density which could actively participate in the transient collision process. This would result in more enhancement of k_1/k_c in cells and buds compared to vesicles.

Fourth, the data summarized in Table IV show that DLPC rate coefficients do not change much with pH. However, for DMPC, k_1 does not change, but k_c increases with decreasing pH. Therefore, the predominant mechanism in DMPC transfer varies with experimental conditions, with transfer in collisional complexes becoming more important at low pH. At very low donor vesicle concentrations (inset, Figure 1a), however, the transient collision term is negligible, and DMPC transfer becomes pH-independent. In addition, pH-induced acceleration of lipid transfer was not observed between small unilamellar PC vesicles. Therefore, the increase in the transient collision transfer at low pH may reflect titration of cell-surface components. The erythrocyte surface is known to be densely studded with carbohydrate, either as glycolipid or as glycoprotein (Viitala & Järnefelt, 1985). Both desialiation and Pronase treatment accelerate DMPC transfer 1.5–2-fold, consistent with diminished steric barriers to contact. The accelerated lipid transfer at low pH, accordingly, may reflect membrane component patching (Arvinte et al., 1989b) that facilitates productive collisions.

ACKNOWLEDGMENT

We thank Dr. Romita Sen for help with NMR spectroscopy.

REFERENCES

Arvinte, T., & Hildenbrand, K. (1984) *Biochim. Biophys. Acta 775*, 86–94.

Arvinte, T., Schulz, B., Cudd, A., & Nicolau, C. (1989a) *Biochim. Biophys. Acta 981*, 51–60.
Arvinte, T., Cudd, A., Schulz, B., & Nicolau, C. (1989b) *Biochim. Biophys. Acta 981*, 61–68.
Bartlett, G. R. (1959) *J. Biol. Chem. 234*, 466–468.
Bessis, M. (1973) in *Red Cell Shape* (Bessis, M., Weed, R. I., & LeBlond, P. F., Eds.) pp 1–23, Springer-Verlag, New York.
Boggs, J. (1980) *Can. J. Biochem. 58*, 755–770.
Brown, R. E. (1992) *Biochim. Biophys. Acta 1113*, 375–389.
Cabantchik, Z. I., & Rothstein, A. (1974) *J. Membr. Biol. 15*, 207–226.
Daleke, D. L., & Huestis, W. H. (1985) *Biochemistry 24*, 5406–5416.
Daleke, D. L., & Huestis, W. H. (1989) *J. Cell Biol. 108*, 1375–1385.
DeCuyper, M., & Joniau, M. (1985) *Biochim. Biophys. Acta 814*, 374–380.
DeCuyper, M., Joniau, M., & Dangreau, H. (1983) *Biochemistry 22*, 415–420.
Duckwitz-Peterlein, G., Eilenberger, G., & Overath, P. (1977) *Biochim. Biophys. Acta 469*, 311–325.
Elgsaeter, A., Shotton, D. M., & Branton, D. (1976) *Biochim. Biophys. Acta 426*, 101–122.
Fairbanks, G., Steck, T. L., & Wallach, D. F. H. (1971) *Biochemistry 10*, 2606–2617.
Ferrell, J. E., Jr., Lee, K.-J., & Huestis, W. H. (1985a) *Biochemistry 24*, 2849–2857.
Ferrell, J. E., Jr., Lee, K.-J., & Huestis, W. H. (1985b) *Biochemistry 24*, 2857–2864.
Fugler, L., Clejan, S., & Bittman, R. (1985) *J. Biol. Chem. 260*, 2498–4102.
Fullington, D., Shoemaker, D. G., & Nichols, J. W. (1990) *Biochemistry 29*, 879–886.
Gardam, M. A., Itovitch, J. J., & Silvius, J. R. (1989) *Biochemistry 28*, 884–893.
Garnier-Suillerot, A., & Gattegno, L. (1988) *Biochim. Biophys. Acta 936*, 50–60.
Gokhale, K. M., & Metha, N. G. (1987) *Biochem. J. 241*, 505–511.
Gurd, E. R. N. (1960) in *Lipid Chemistry* (Hanahan, D. J., Ed.) pp 208–259, Wiley, New York.
Haberland, M. E., & Reynolds, J. A. (1975) *J. Biol. Chem. 250*, 6636–6639.
Hauser, H., & Phillips, M. C. (1979) *Prog. Surf. Membr. Sci. 13*, 297–414.
Huang, C. (1969) *Biochemistry 8*, 344–351.
Jones, D. J., & Thompson, T. E. (1989) *Biochemistry 28*, 129–134.
Jones, D. J., & Thompson, T. E. (1990) *Biochemistry 29*, 1593–1600.
Lelkes, G., & Fodor, I. (1991) *Biochim. Biophys. Acta 1065*, 135–144.
Martin, F. J., & MacDonald, R. C. (1976) *Biochemistry 15*, 321–327.
Massari, S., Folena, E., Ambrosin, V., Schiavo, G., & Colonna, R. (1991) *Biochim. Biophys. Acta 1067*, 131–138.
Massey, J. B., Gotto, A. M., Jr., & Pownall, H. J. (1982) *J. Biol. Chem. 257*, 5444–5448.
McLean, L. R., & Phillips, M. C. (1981) *Biochemistry 20*, 2893–2900.
McLean, L. R., & Phillips, M. C. (1984a) *Biochemistry 23*, 4624–4630.
McLean, L. R., & Phillips, M. C. (1984b) *Biochim. Biophys. Acta 776*, 21–26.
Nichols, J. W. (1988) *Biochemistry 27*, 3925–3931.
Nichols, J. W., & Pagano, R. E. (1981) *Biochemistry 20*, 2783–2789.
Othmane, A., Bitol, M., Snabre, P., & Mills, P. (1990) *Eur. Biophys. J. 18*, 93–99.
Papahadjoloulos, D., Hui, S., Vail, W. J., & Poste, G. (1976) *Biochim. Biophys. Acta 448*, 245–264.
Phillips, M. C., Johnson, W. J., & Rothblat, G. H. (1987) *Biochim. Biophys. Acta 906*, 223–276.
Rand, R. P., & Parsegian, V. A. (1986) *Annu. Rev. Physiol. 48*, 201–212.
Roseman, M. A., & Thompson, T. E. (1980) *Biochemistry 19*, 439–444.
Steck, T. L., Keady, F. J., & Lange, Y. (1988) *J. Biol. Chem. 263*, 13023–13031.
Stockton, G. W., Polnaszek, C. F., Leitch, L. C., Tulloch, A. P., & Smith, I. C. P. (1974) *Biochem. Biophys. Res. Commun. 60*, 844–850.
Tanaka, K.-I., & Ohnishi, S.-I. (1976) *Biochim. Biophys. Acta 426*, 218–231.
Tanford, C. (1980) in *The Hydrophobic Effect*, 2nd ed., Wiely, New York.
Thomas, P. D., & Poznansky, M. J. (1988) *Biochem. J. 254*, 155–160.
Träuble, H., & Eibl, H. (1974) *Proc. Natl. Acad. Sci. U.S.A. 71*, 214–219.
Viitala, J., & Järnefelt, J. (1985) *Trends Biochem. Sci. 10*, 392–395.
Weltzien, H. U. (1979) *Biochim. Biophys. Acta 559*, 259–287.
Williamson, P., Algarin, L., Bateman, J., Choe, H.-R., & Schlegel, R. A. (1985) *J. Cell. Physiol. 123*, 209–214.
Wimley, W. C., & Thompson, T. E. (1991) *Biochemistry 30*, 4200–4204.
Zlatkis, A., Zak, B., & Boyle, A. J. (1953) *J. Lab. Clin. Med. 41*, 486–492.